ROA in other spectral regions of this molecule and in other molecules. In particular, we have presented evidence for the importance of vibrational mixing of ring motions of similar frequency but different symmetry species induced by chiral substitution and coupling with motions of the substituent. It seems probable that, as is observed in VCD, intense ROA arises from nuclear motion spread out over the chiral frame, rather than from localized vibrations. For example, the prominent ROA couplet observed at 968 and 942 cm^{-1} in 3-methylcyclohexanone[2] (corresponding to Raman bands at 969, 960, and 946 cm^{-1}) lies in the frequency region for the A′ methyl rock in methylcyclohexane[24] (971 cm^{-1}) and for the cyclohexanone[19] modes at 990 (A′) and 907 cm^{-1} (A″) which involve C–C stretch and CCH deformation in the ring. The ROA couplet probably arises from chiral vibrational mixing of these modes, rather than from mixing of the A′ and A″ methyl rocks as has been previously proposed.[3,18] The couplet near 1450 cm^{-1} in 1-substituted arylethanes,[4,5,30–32] another important example, lies in the region where both the two components of the antisymmetric methyl deformation and two substituted benzene modes, 19a (a_1) and 19b (b_2) in Wilson's notation,[33] occur. The couplet is absent both in trideuterio-[8] or trifluoro-substituted[32] species and in (*p*-bromophenyl)ethylamine.[32] As previously suggested,[32] a dynamic interaction of the methyl and phenyl modes is require to explain the ROA couplet, rather than static splitting of the methyl degeneracy.[4] Hug[5] postulated either an equal admixture of the 19b mode with the two methyl deformations or a biphasic coupling of 19b with one of the methyl deformation components. Since all four modes in this region can interact, a couplet generated by methyl deformation mixed with in-phase contributions of 19b and 19a and a second methyl deformation coupled to out-of-phase 19a, 19b contributions is also a possible explanation, in line with our 3-methylcyclohexanone results. Similarly, the substituted benzene modes 17a (a_2) and 17b (b_1) interacting with the methyl rock or the modes 16a (a_2) and 16b (b_1) interacting with chiral substituent motion are types of chirally induced mixing which may give rise to the ROA features near 1000 cm^{-1} and 450 cm^{-1} in chirally substituted arylethanes.

This study also points to the usefulness of stereoprojections of vibrational displacements in identifying patterns of motion and coupling in the normal modes of large, low-symmetry molecules. We note, in particular, that symmetry reduction need not drastically alter the form of vibrational motion.

Finally, we have presented the first theoretical calculation of ROA intensity which agrees well with experiment over a fairly large spectral region. The ADI and bond polarizability models may also yield good results given an accurate force field, but we emphasize here that, unlike these two models, the ROA–APT model requires no empirical parameters once a molecular orbital scheme has been chosen. Furthermore, the ROA–APT model does not require division of the molecule into local polarizability units. Hopefully, correlation between 3-methylcyclohexanone, methylcyclohexane, and cyclohexanone spectra will also aid in the interpretation of the more complex mid-infrared and Raman regions (1750–700 cm^{-1}) in which both ROA and FTIR–VCD[34] data for 3-methylcyclohexanone have been recorded, and in which the APT models of both ROA and VCD can be simultaneously employed and evaluated.

Acknowledgment is given for financial support of this research by grants from the National Institutes of Health, GM-23567, and the National Science Foundation, CHE-83-02416.

---

(30) Barron, L. D. *Nature (London)* **1975**, *255*, 458.
(31) Barron, L. D.; Clark, B. P. *J. Chem. Res. Suppl.* **1979**, *36*.
(32) Barron, L. D. *J. Chem. Soc., Perkin Trans. 2* **1977**, 1790.
(33) Dollish, F. R.; Fateley, W. G.; Bentley, F. F. "Characteristic Raman Frequencies of Organic Compounds"; Wiley: New York, 1974; Chapter 13.
(34) Lipp, E. D.; Zimba, C. G.; Nafie, L. A. *Chem. Phys. Lett.* **1982**, *90*, 1.

Gas-Phase Reactions of FeO^+ with Hydrocarbons

T. C. Jackson, D. B. Jacobson, and B. S. Freiser*

Contribution from the Department of Chemistry, Purdue University, West Lafayette, Indiana 47907. *Received August 15, 1983*

Abstract: The reactions of FeO^+ with linear alkanes, cyclic alkanes, and branched alkanes are presented. In general from the reactions observed, it appears that FeO^+ is more reactive toward alkanes than Fe^+ which is due mainly to the greater reaction exothermicity involved in H_2O loss. The majority of the products observed may be explained by initial C–H insertion and loss of H_2O to produce an activated Fe^+–olefin complex which subsequently decomposes. An alternative mechanism involving C–C insertion, however, cannot be ruled out and is in fact supported by observation of radical loss products. These radical loss products dominate for systems in which C–H insertion pathways are inhibited by the absence of β hydrogens.

While transition-metal ion chemistry has been extensively studied in solution, only recently has much attention been given to the gas-phase chemistry of these species. These recent studies on the reactions of gas-phase transition-metal ions with various organic compounds have shown this chemistry to be both rich and unusual, exhibiting oxidative addition across carbon–halogen,[1–3] carbon–oxygen,[2,4,5] carbon–hydrogen,[2,6–9] and carbon–carbon[2,6–9] bonds. In addition, these studies have resulted in kinetic, mechanistic, and thermodynamic data about the metal ions themselves, and also about the reactions in which they take part. A major focus of these studies has been the determination of reaction mechanisms, and this has been greatly facilitated by the

---

(1) Allison, J.; Ridge, D. P. *J. Am. Chem. Soc.* **1976**, *98*, 7445.
(2) Allison, J.; Ridge, D. P. *J. Am. Chem. Soc.* **1979**, *101*, 4998.
(3) Uppal, J. S.; Staley, R. H. *J. Am. Chem. Soc.* **1980**, *102*, 4144.
(4) Allison, J.; Ridge, D. P. *J. Am. Chem. Soc.* **1978**, *100*, 163.
(5) Burnier, R. C.; Byrd, G. D.; Freiser, B. S. *J. Am. Chem. Soc.* **1981**, *103*, 4360.
(6) (a) Allison, J.; Freas, R. B.; Ridge, D. P. *J. Am. Chem. Soc.* **1979**, *101*, 1332. (b) Freas, R. B.; Ridge, D. P. *Ibid.* **1980**, *102*, 7129.
(7) (a) Armentrout, P. B.; Beauchamp, J. L. *J. Am. Chem. Soc.* **1981**, *103*, 784. (b) Halle, L. F.; Armentrout, P. B.; Beauchamp, J. L. *Organometallics* **1982**, *1*, 963.
(8) (a) Byrd, G. D.; Burnier, R. C.; Freiser, B. S. *J. Am. Chem. Soc.* **1982**, *104*, 3565. (b) Byrd, G. D.; Freiser, B. S. *Ibid.* **1982**, *104*, 5944.
(9) (a) Jacobson, D. B.; Freiser, B. S. *J. Am. Chem. Soc.* **1983**, *105*, 736. (b) Jacobson, D. B.; Freiser, B. S. *Ibid.* **1983**, *105*, 5197.

0002-7863/84/1506-1252$01.50/0

determination of product ion structures via such methods as collision-induced dissociation[6b,9] (CID), specific ion-molecule reactions,[9,10] and the use of labeled compounds in the reactions.[10] Thermochemical data relating to metal-hydrogen and metal-methyl ion complexes, obtained in an ion-beam instrument, have also been valuable in postulating reasonable reaction mechanisms.[7,11]

When studying metal ions in solution, one of the predominant factors affecting the chemistry is that caused by the ligands around the metal. This effect has been extensively studied and is understood to a reasonable degree. In the gas phase, however, only a few studies of coordinated metal ions have been reported.[2,4,6b] While the reactions of many bare metal ions remain to be investigated, techniques are available for the generation and study of specifically coordinated metal ions in the gas phase. Given the scope of current inorganic research involving metal-ligand complexes, it is essential to begin to delineate the effect of ligands on the reactions of gas-phase metal ions. Such studies will yield the intrinsic effect of a single ligand in the absence of additional ligands and complicating solvent effects. Future studies will involve investigating the effect of sequentially adding ligands, while a comparison of the gas- and solution-phase results will ultimately provide a measure of how important a role the solvent does play.

In this paper we report the reactions of gas-phase FeO^+ with small hydrocarbons and compare these reactions with those of Fe^+ to determine the differences in reactivity caused by the addition of the oxygen ligand. The catalytic properties of both iron and its oxides are well known and have been reasonably well studied. In addition, iron is an important element with both its solution-phase and gas-phase chemistries well studied. For these reasons FeO^+ was a good candidate for this work.

Experimental

All experiments were performed on a prototype Nicolet FTMS-1000 mass spectrometer, which has been previously described in detail[12] and is equipped with a 5.2-cm cubic trapping cell situated between the poles of a Varian 15-in. electromagnet maintained at 0.9 T. The cell has a $^1/_4$-in. hole in one of the transmitter plates permitting irradiation of the interior of the cell with various light sources. Fe^+ was generated by focusing the beam of a Quanta Ray ND:YAG laser, frequency doubled to 530 nm, onto the opposite receiver plate which supported a high purity thin iron foil. Details of the laser ionization experiment have been described elsewhere.[5,8]

FeO^+ was generated by trapping Fe^+ in the presence of N_2O. These two species react to form FeO^+ and N_2.[13] The N_2O was admitted to the cell through a General Valve Corp. Series 9 pulsed solenoid valve. Details of the pulsed valve experiment are described elsewhere.[14] Pulsing in the reagent gas allows the system to be maintained at a lower pressure during the majority of the reaction sequence which enables ions to be trapped for a longer period of time, and also eliminates further reactions with N_2O.

The distribution of the listed product ions is reproducible to within ±10%. Product distributions of subsequent reactions were determined by using swept double resonance ejection techniques[15] to isolate the ion of interest. These ions were then allowed to react further, and the products were subsequently detected.

Details of the CID experiments have previously been discussed.[9,12] The collisional energy of the ions can be varied, typically between 0 and 100 eV, from which plots of CID product ion intensities vs. collision energy can be produced. The distribution of the kinetic energies is dependent on the total average kinetic energy and is approximately 35% at 1 eV, 10% at 10 eV, and 5% at 30 eV.[16] Simple metal ion complexes can unambiguously be assigned structures via CID.[9] Complexes containing ligands possessing five or more carbon atoms, however, can undergo facile rearrangements which may yield CID spectra that are not very diagnostic. Therefore, while CID spectra of major product ions were obtained, many of the structures are necessarily assigned as "reasonable" as opposed to proven.

Table I. The Percentages of the Neutral Products Lost in the Primary Reactions of Fe^+ and FeO^+ with Linear Alkanes (For Each Reaction the Trapping Time Was ~500 ms and the Pressure Was ~2×10^{-7} torr)

	$Fe^{+\,a}$		FeO^+	
alkane	neutral lost	% of total	neutral lost	% of total
CH_4	NR		NR	
C_2H_6	NR		H_2O	70
			C_2H_4	20
			H_2O, C_2H_4	10
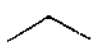	CH_4	76	H_2O	50
	H_2	24	$CH_3\cdot$	20
			H_2O, C_3H_6	20
			C_3H_6	10
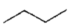	C_2H_6	60	H_2O, H_2	60
	CH_4	29	H_2O, C_2H_4	30
	H_2	8	H_2O, C_4H_8	10
	$2H_2$	3		
	C_3H_8	43	H_2O, C_2H_4	44
	CH_4	22	H_2O, C_3H_6	27
	H_2	16	H_2O, CH_4	15
	C_2H_6	15	$CH_3CH_2\cdot$	9
	CH_4, H_2	4	H_2O, C_5H_{10}	5
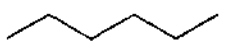	C_4H_{10}	31	H_2O, C_3H_6	34
	H_2	27	H_2O, C_2H_4	21
	CH_4	13	$H_2O, 3H_2$	15
	C_3H_8	11	$CH_3CH_2\cdot$	14
	C_2H_6	11	H_2O, C_2H_4, H_2	9
	C_2H_6, H_2	7	H_2O, C_4H_8	7

[a] Data for Fe^+ taken from ref 9b.

Table II. The Percentages of the Neutral Products Lost in the Primary Reactions of Fe^+ and FeO^+ with Cyclic Alkanes (For Each Reaction the Trapping Time Was ~500 ms and the Pressure Was ~2×10^{-7} torr)

	$Fe^{+\,a}$		FeO^+	
alkane	neutral lost	% of total	neutral lost	% of total
	NR		NR	
	C_2H_4	95	C_2H_4	53
	H_2	5	C_2H_4O	19
			H_2O, C_4H_6	16
			H_2O	12
	H_2	65	H_2O, H_2	100
	$2H_2$	34		
	C_2H_4	1		
	H_2	63	$H_2O, 2H_2$	100
	$2H_2$	24		
	$3H_2$	13		
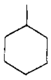	H_2	21	$H_2O, 2H_2$	65
	$2H_2$	18	H_2O, CH_4, H_2	35
	$3H_2$	29		
	CH_4	2		
	H_2, CH_4	6		
	$2H_2, CH_4$	24		

[a] Data for Fe^+ taken from ref 18.

Chemicals were obtained in high purity from commercial sources and used as supplied except for multiple freeze-pump-thaw cycles to remove

---

(10) Halle, L. F.; Houriet, R.; Kappes, M.; Staley, R. H.; Beauchamp, J. L. *J. Am. Chem. Soc.* **1982**, *104*, 6293.

(11) (a) Armentrout, P. B.; Beauchamp, J. L. *Chem. Phys.* **1980**, *50*, 37. (b) Armentrout, P. B.; Beauchamp, J. L. *J. Chem. Phys.* **1981**, *74*, 2819. (c) Armentrout, P. B.; Halle, L. F.; Beauchamp, J. L. *J. Am. Chem. Soc.* **1981**, *103*, 6499.

(12) (a) Cody, R. B.; Freiser, B. S. *Int. J. Mass Spectrum. Ion Phys.* **1982**, *41*, 199. (b) Cody, R. B.; Burnier, R. C.; Freiser, B. S. *Anal. Chem.* **1982**, *54*, 96.

(13) Kappes, M. M.; Staley, R. H. *J. Phys. Chem.* **1981**, *85*, 942.

(14) Carlin, T. J.; Freiser, B. S. *Anal. Chem.* **1983**, *55*, 571.

(15) (a) Comisarow, M. B.; Grassi, V.; Parisod, G. *Chem. Phys. Lett.* **1978**, *57*, 413. (b) Marshall, A. G.; Comisarow, M. B.; Parisod, G. *J. Chem. Phys.* **1979**, *71*, 4434. (c) Parisod, G.; Comisarow, M. B. *Adv. Mass Spectrum.* **1979**, *8A*, 212.

(16) Huntress, W. T.; Mosesman, M. M.; Elleman, D. D. *J. Chem. Phys.* **1971**, *54*, 843.

Table III. The Percentages of the Neutral Products Lost in the Primary Reactions of Fe^+ and FeO^+ with Branched Alkanes (For Each Reaction the Trapping Time Was ~500 ms and the Pressure Was ~2 × 10^{-7} torr)

	Fe^{+} [a]		FeO^+	
alkane	neutral lost	% of total	neutral lost	% of total
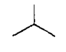	CH_4 H_2	46 54	$CH_3\cdot$ H_2O	65 35
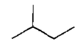	CH_4 H_2 $H_2 + CH_4$ C_2H_6 C_3H_8 $2H_2$	27 24 22 20 4 3	H_2O, C_2H_4 H_2O, CH_4 $CH_3\cdot$ H_2O, C_3H_6 H_2O, H_2 $CH_3CH_2\cdot$ $H_2O, CH_3\cdot$	32 22 14 12 10 5 5
	CH_4	100	$CH_3\cdot$ $H_2O, CH_3\cdot$ $OFeCH_3$ or $C_5H_9\cdot, H_2O$	65 25 10
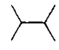	H_2 C_3H_8 CH_4 C_2H_6 C_4H_{10} $2H_2$ CH_4, H_2 C_2H_6, H_2	5 13 6 7 1 8 38 22	H_2O, C_3H_6 $CH_3\cdot$ H_2O, CH_4 $(CH_3)_2CH\cdot$	47 24 23 6
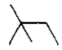	C_2H_6 C_3H_8 CH_4 C_4H_{10} H_2 CH_4, H_2 C_2H_6, H_2	62 6 8 4 3 6 10	$CH_3\cdot$ H_2O, C_2H_4 $CH_3CH_2\cdot$ $C_5H_{11}O$ $H_2O, CH_3\cdot$ H_2O, CH_4 $H_2O, C_6H_{11}\cdot$ $H_2O, C_4H_7\cdot$ $H_2, CH_3\cdot$ H_2O, C_4H_8	26 24 18 7 7 5 4 3 3 3
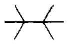	$2CH_4$ or C_2H_6, H_2 C_4H_{10} CH_4 $H_2, C_3H_8, CH_4, C_2H_6$ C_3H_8 H_2	71 8 8 6 5 2	$CH_3\cdot$ $(CH_3)_3C\cdot$ H_2O, C_4H_8 $H_2O, CH_3\cdot$	38 28 20 14

[a] Data for Fe^+ taken from: Halle, L. F.; Armentrout, P. B.; Beauchamp, J. L. *Organometallics*, **1982**, *1*, 963.

Table IV. Relevant Bond-Dissociation Energies and Heats of Formation

	kcal/mol	ref		kcal/mol	ref
$D(Fe^+ - H)$	58	*a*	$D(CH_3 - H)$	104	*b*
$D(Fe^+ - CH_2)$	96	*a*	$D(C_2H_5 - H)$	98	*b*
$D(Fe^+ - CH_3)$	69	*a*	$D(n\text{-}C_3H_7 - H)$	98	*b*
$D(Fe^+ - C_2H_4)$	33	18	$D(\text{allyl} - H)$	89	*d*
$D(Fe^+ - O)$	68	*a*	$D(O - C)$	86	*d*
			$D(C - OR)$	82	*d*
$\Delta H_f(Fe^+)$	280.4	*b*	$D(RO - H)$	99	*d*
$\Delta H_f(FeCH_2^+)$	278	*c*	$D(CH_3 - OH)$	91.3	*b*
$\Delta H_f(FeCH_3^+)$	246	*c*	$D(C_2H_5 - OH)$	91.2	*b*
$\Delta H_f(FeC_2H_4^+)$	256	*c*	$\Delta H_f(H)$	52.1	*b*
$\Delta H_f(FeO^+)$	272	*c*	$\Delta H_f(CH_2)$	93.7	*b*
			$\Delta H_f(CH_3)$	34.0	*b*
			$\Delta H_f(C_2H_5)$	25.7	*b*
			$\Delta H_f(CH_4)$	-17.9	*b*
			$\Delta H_f(C_2H_6)$	-20.2	*b*
			$\Delta H_f(C_2H_4)$	12.5	*b*
			$\Delta H_f(CH_3OH)$	-48.0	*b*
			$\Delta H_f(C_2H_5OH)$	-56.2	*b*
			$\Delta H_f(O)$	59.6	*b*

[a] Halle, L. F.; Armentrout, P. B.; Beauchamp, J. L. *Organometallics*, **1982**, *1*, 963. [b] Rosenstock, H. M.; Draxl, K.; Steiner, B. W.; Herron, J. T. *J. Phys. Chem. Ref. Data Suppl.*, **1977**, *6*. Values either directly obtained or calculated from other values given. [c] Calculated from the bond-dissociation data given in the Table. [d] McMillen, D. F.; Golden, D. M. *Annu. Rev. Phys. Chem.* **1982**, *33*, 493–532.

noncondensible gases. Sample pressures were on the order of 2 × 10^{-7} torr. Argon was used as the collision gas at a total pressure (sample plus argon) of approximately 5 × 10^{-6} torr. A Bayard-Alpert ionization gauge was used to monitor pressures.

Results and Discussion

The reactions of FeO^+ with linear alkanes, cyclic alkanes, and branched alkanes are presented in Tables I, II, and III, respectively. All of the heats of reaction given in the text were calculated on the basis of the thermodynamic values in Table IV.

In general from the reactions observed, it appears that FeO^+ is more reactive toward alkanes than Fe^+ which is due mainly to the greater reaction exothermicity involved in H_2O loss. The majority of the products observed may be explained by initial C–H insertion and loss of H_2O to produce an activated Fe^+–olefin complex which subsequently decomposes. An alternative mechanism involving C–C insertion, however, cannot be ruled out and is in fact supported by observation of radical loss products. These radical loss products dominate for systems in which C–H insertion pathways are inhibited by the absence of β hydrogens.

Linear Alkanes. The reactions of FeO^+ with the linear alkanes from methane to hexane are summarized in Table I. For comparison the results of the reactions of Fe^+ with the same alkanes are also included. Neither FeO^+ nor Fe^+ reacts with methane, and while generation of $FeCH_2^+$ from Fe^+ is calculated to be endothermic, its generation from FeO^+ would be highly exothermic. The absence of $FeCH_2^+$ may, therefore, be a manifestation of the fact that α-hydrogen transfers are unfavorable even though all of the intermediates appear to be energetically accessible on the basis of the bond-dissociation energies in Table IV. This result could suggest, however, that these bond energies are altered substantially by the presence of other ligands; i.e., the bond energies are not simply additive. An alternative pathway is suggested by reaction 1 reported by Ridge et al.,[2] but the analogous reaction is not observed for FeO^+ and CH_4.

$$Fe^+ + CH_3OH \rightarrow FeOH^+ + CH_3\cdot \qquad (1)$$

Scheme I

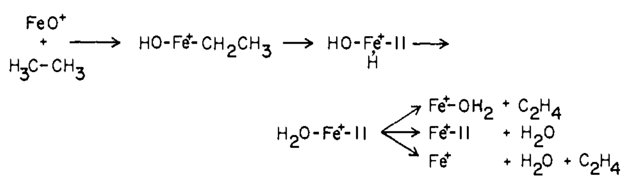

While Fe^+ fails to react with ethane, FeO^+ reacts to give the products shown in reactions 2–4. Each of these pathways is highly

$$FeO^+ + C_2H_6 \xrightarrow{70} FeC_2H_4^+ + H_2O \qquad (2)$$

$$\xrightarrow{20} FeH_2O^+ + C_2H_4 \qquad (3)$$

$$\xrightarrow{10} Fe^+ + C_2H_4 + H_2O \qquad (4)$$

exothermic and, in particular, formation of $FeC_2H_4^+$ by reaction 2 is estimated to be 51 kcal/mol exothermic as compared to near thermoneutral for its formation from Fe^+ and C_2H_6 via loss of H_2. A mechanism for reactions 2–4 is shown in Scheme I in which FeO^+ inserts into a C–H bond resulting in the formation of a hydroxy–iron–ethyl intermediate. Direct insertion of the FeO group into the C–H bond can be envisioned as occurring via a four-centered intermediate, but initial insertion of Fe followed by hydrogen migration onto the oxygen cannot be ruled out. Following formation of the hydroxy intermediate, β-hydride transfer occurs from ethyl to the metal followed by rearrangement to form the water–iron–ethene complex, which can then eliminate either or both ligands to form the products indicated. In the

Scheme II

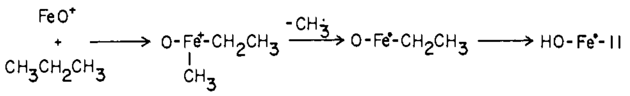

Scheme III

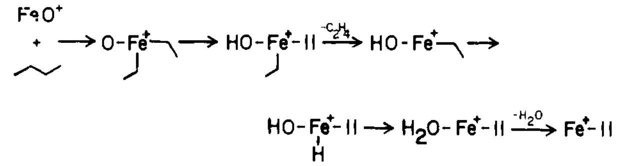

reaction of Fe^+ and ethanol, the same hydroxy intermediate as in Scheme I is formed.[2] The energy available, however, is far less and only reaction 5 is observed which is about 23 kcal/mol exothermic. Finally, Fe^+ reacts with dimethyl ether to produce

$$Fe^+ + C_2H_5OH \rightarrow FeC_2H_4^+ + H_2O \qquad (5)$$

$Fe(CH_2O)^+$ exclusively.[5] The absence of this product from the reaction of FeO^+ with ethane suggests that at no time is a methyl–iron–methoxy intermediate produced.

Propane reacts with FeO^+ to give the products shown in reactions 6–9. While the products in reactions 6–8 can be explained

$$FeO^+ + C_3H_8 \xrightarrow{50} FeC_3H_6^+ + H_2O \qquad (6)$$

$$\xrightarrow{10} FeH_2O^+ + C_3H_6 \qquad (7)$$

$$\xrightarrow{20} Fe^+ + H_2O + C_3H_6 \qquad (8)$$

$$\xrightarrow{20} HO\text{-}Fe^+\text{-}C_2H_4 + CH_3\cdot \qquad (9)$$

by initial C–H insertion in a manner similar to that shown in Scheme I, the $CH_3\cdot$ loss product in reaction 9 is unexpected and apparently arises from an initial C–C insertion (Scheme II). Collision-induced dissociation on the product ion from reaction 9 results in predominantly ethene loss in accord with the hydroxy–iron–ethene structure. As shown in Scheme II, $CH_3\cdot$ loss must occur prior to a β-hydride shift from the ethyl group since, otherwise, CH_4 or C_2H_4 loss would be observed.

The reactions of FeO^+ with butane are shown in reactions 10–12. The highly exothermic nature of these reactions is reflected in the fact that only multiple loss products are observed.

$$FeO^+ + n\text{-}C_4H_{10} \xrightarrow{60} FeC_4H_6^+ + H_2O + H_2 \qquad (10)$$

$$\xrightarrow{30} FeC_2H_4^+ + H_2O + C_2H_4 \qquad (11)$$

$$\xrightarrow{10} Fe^+ + (C_4H_6 + H_2O + H_2) \text{ or } (H_2O + 2C_2H_4) \qquad (12)$$

Reaction by Scheme I would predict the formation of an Fe^+–butene complex. Activated Fe^+–butene complexes readily lose H_2 to form Fe^+–butadiene.[17] That no Fe^+–butene is observed and only Fe^+–butadiene is seen indicates that a considerable amount of excess energy is present upon the initial formation of Fe^+–butene. The formation of $FeC_2H_4^+$ is postulated as arising from insertion into the central C–C bond, followed by elimination of ethene and water from the complex (Scheme III). It is not clear at this point why $C_2H_5\cdot$ loss is not observed from the intermediate in Scheme III.

Pentane and hexane react to form a number of products. The majority of the products may be explained by initial C–H insertion and loss of H_2O (Scheme I) to produce an activated Fe^+–olefin complex. This complex then dissociates by similar channels reported by Jacobson and Freiser for CID on Fe^+–pentene and Fe^+–hexene.[17] Alternatively, many of the products could be derived by initial C–C insertion, Scheme III. The high percentage of $C_2H_5\cdot$ loss for both pentane and hexane is again surprising and provides evidence for at least some C–C insertion.

Cyclic Alkanes. The disparity between the reactivity of Fe^+ and FeO^+ is emphasized in the reactions of cyclic alkanes, which are summarized in Table II. Neither ion reacts with cyclopropane. Cyclobutane reacts as shown in reactions 13–16. The major product formed, $FeC_2H_4O^+$, is interesting in that CID of this ion shows exclusive loss of C_2H_4O. This suggests that the C_2H_4O is in fact a single ligand, either acetaldehyde or ethylene oxide.

$$FeO^+ + \text{cyclobutane} \xrightarrow{53} Fe(OC_2H_4)^+ + C_2H_4 \qquad (13)$$

$$\xrightarrow{19} FeCH^+ + C_2H_4O \qquad (14)$$

$$\xrightarrow{16} Fe^+ + (C_2H_4 + C_2H_4O) \text{ or } (H_2O + C_4H_6) \qquad (15)$$

$$\xrightarrow{12} FeC_4H_6^+ + H_2O \qquad (16)$$

This species could result from a mechanism similar to that proposed for the reaction of Fe^+, in which the iron inserts into one of the C–C bonds of cyclobutane and forms either a butadiene ligand or two ethene ligands.[18] In the process of forming the ethene ligands with FeO^+, the oxygen becomes incorporated forming a C_2H_4O and an ethene ligand, rather than an oxygen and two ethene ligands. After formation of the two-ligand complex, one or both of the ligands are eliminated. Formation of the butadiene ligand is also seen.

Cyclopentane reacts with FeO^+ to give exclusively Fe^+–cyclopentadiene which reacts further by loss of $2H_2$ and $3H_2$ to form $Fe(C_5H_6)_2^+$ and $Fe(C_5H_5)_2^+$, respectively, as reported previously.[18] Formation of Fe^+–cyclopentadiene is again consistent with first eliminating H_2O leaving an activated Fe–cyclopentene$^+$ which eliminates H_2.

With cyclohexane, FeO^+ gives exclusively the triple dehydrogenation product, the Fe^+–benzene ion, while Fe^+ gives products with one, two, and three dehydrogenations.[18] Finally, with methylcyclohexane, FeO^+ reacts to give an Fe^+–toluene complex and also the Fe^+–benzene ion. Fe^+ gives these products, in addition to less dehydrogenated species.

Thus for cyclic alkanes, FeO^+ promotes reactions, especially dehydrogenations, to a greater extent than does Fe^+, while maintaining similar reaction channels. Again, this is consistent with elimination of H_2O leaving an activated species which can then follow CID elimination pathways to further eliminate one or more molecules of H_2.

Branched Alkanes. It is with branched alkanes that the chemistry of FeO^+ becomes the most interesting, exhibiting C–C bond insertion and predominant radical loss. In the reaction with 2-methylpropane, two products are observed (reactions 17 and 18). The predominant product is that produced from the loss of $CH_3\cdot$.

$$FeO^+ + CH_3CH(CH_3)CH_3 \xrightarrow{65} HO\text{—}Fe^+\text{—}C_3H_6 + CH_3\cdot \qquad (17)$$

$$\xrightarrow{35} Fe(i\text{-}C_4H_8)^+ + H_2O \qquad (18)$$

An equilibrium may exist between the propene and the hydrido–π-allyl complex, reaction 19. The hydrido–π-allyl complex

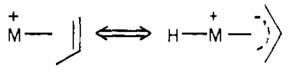

(19)

was postulated for Rh$^+$,[8b] for example, but evidence suggested the presence of only a propene complex for Fe^+.[9b] An analogous equilibrium may exist for the FeO^+ case, reaction 20, but ace-

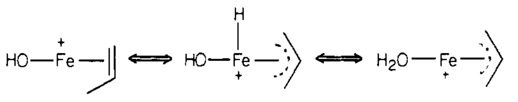

(20)

---

(17) Jacobson, D. B.; Freiser, B. S. *J. Am. Chem. Soc.* **1983**, *105*, 7484.

(18) Jacobson, D. B.; Freiser, B. S. *J. Am. Chem. Soc.* **1983**, *105*, 7492.

(19) Kappes, M. M.; Staley, R. H. *J. Am. Chem. Soc.* **1981**, *103*, 1286.

Scheme IV

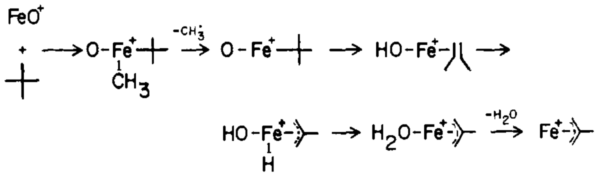

tonitrile is observed to displace only propene from the ion produced in reaction 17 suggesting a stable and nonequilibrating hydroxypropene structure. Since the iron–π-allyl complex is observed as one of the CID products from the ion produced in reaction 17, however, the aquo–iron–π-allyl complex must be an easily accessed activated complex.

FeO^+ reacts with 2,2-dimethylpropane to produce two major products, reactions 21 and 22. In this case if FeO^+ inserts into

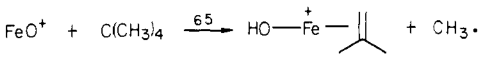 (21)

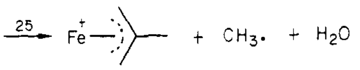 (22)

a C–H bond, there are no β hydrogens present to shift onto the metal. Thus, the possible pathways involving β-hydride shifts are closed to these reactants and they are not observed. Formation of the product in reaction 21 is postulated to occur via insertion into a C–C bond, followed by elimination of the methyl radical and a β-hydride shift to form the hydroxy–iron–alkene complex (Scheme IV). In analogy to the product ion formed in reaction 17, this complex can undergo a further hydride shift to form the aquo–iron–π-allyl complex which can then eliminate water (Scheme IV). CID of the product ion in reaction 21 supports the proposed structure, showing a loss of water via a rearrangement at low energy to give the iron–π-allyl complex; at higher energy the alkene ligand is lost, and at yet higher energies, a loss of both ligands is observed (Figure 1). Finally, acetonitrile is observed to displace isobutene from the ion produced in reaction 21, further confirming the hydroxy structure.

The other branched C_5H_{12} isomer is 2-methylbutane. Since this molecule is not as symmetric as 2,2-dimethylpropane, and it also possesses hydrogens β to all of the hydrogen attack positions, the chemistry exhibited is much more varied than that seen for 2,2-dimethylpropane. The major products of the reaction of this compound with FeO^+ are listed in reactions 23–28. All of the

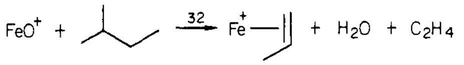 (23)

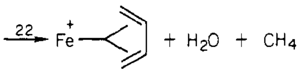 (24)

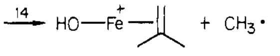 (25)

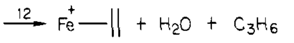 (26)

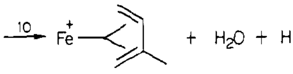 (27)

$\xrightarrow{10}$ other products (see table III) (28)

products involving water loss may readily be explained by initial C–H insertion followed by H_2O loss to form an activated C_5H_{10}–Fe^+ which, as reported previously,[17] can eliminate H_2, CH_4, C_2H_4, and C_3H_6.

Products from reactions 23–26 could, alternatively, result from C–C bond insertion. The Fe^+–propene and Fe^+–ethene products could, for example, arise by insertion into the central C_2–C_3 bond of the molecule, followed by elimination of water and one alkene ligand from the molecule. Elimination of water and ethene would lead to the iron–propene complex, while elimination of water and propene would lead to the iron–ethene complex. Insertion into

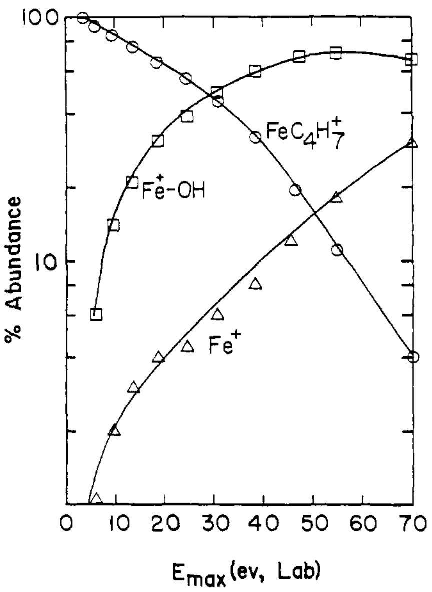

Figure 1. CID product ion intensities vs. kinetic energy for HO—Fe$^+$— generated in reaction 21.

the C_1–C_2 bond of 2-methylbutane would lead, via elimination of methane and loss of water, to the formation of the butadiene complex, reaction 24. The hydroxy–isobutene complex is formed through insertion into the C_3–C_4 bond of the molecule, followed by elimination of the methyl radical and a β-hydride shift. This ion can undergo a further hydride shift and eliminate water to form a π-allyl complex, but this product is seen only in small amounts, as is the formation of a π-allyl complex from the insertion into the C_1–C_2 bond of the compound.

2,3-Dimethylbutane, being a more symmetric molecule than 2-methylbutane, produces a correspondingly smaller number of products (reactions 29–32). The H_2O loss products can again

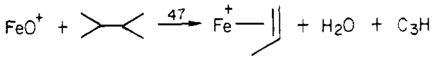 (29)

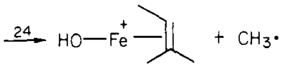 (30)

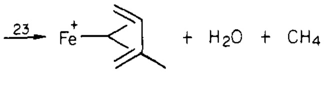 (31)

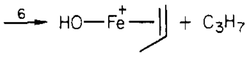 (32)

be explained by an initial C–H insertion mechanism. Alternatively, the major product could result from insertion into the central C–C bond, followed by β-hydrogen transfers to eliminate propene and water. Evidence for this is that a small portion of the intermediate eliminates isopropyl radical and goes on to form the hydroxy–iron–propene ion. Insertion into the terminal C–C bond could explain the formation of the remaining two products. The first is produced via elimination of the methyl radical, followed by β-hydride transfer to form the hydroxy complex. The other is formed by a competitive β-hydride transfer to eliminate methane followed by rearrangements (if necessary) and sequential hydrogen transfer to eliminate water, forming the methylbutadiene–iron ion.

The other branched C_6H_{14} isomer studied, 2,2-dimethylbutane, reacts to form a host of products. Of these, the three major products are shown in reactions 33–35. The first product results from insertion into the C_1–C_2 bond followed by elimination of the methyl radical and a β-hydride shift to form the hydroxy–iron–alkene ion. The other two products listed result from insertion into the central C_2–C_3 bond followed by elimination of the ethyl radical, and a β-hydride shift to form the hydroxy–iron–isobutene ion, or insertion into the C_2–C_3 bond, followed by successive β-hydride shifts to form two alkenes and water attached to the

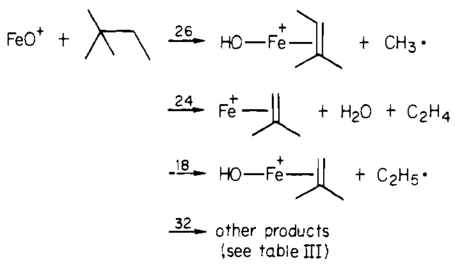

(33)
(34)
(35)
(36)

iron, and completed by elimination of water and ethene to form the iron–isobutene ion. The H_2O elimination product could also arise by initial C–H insertion.

The final compound studied is a highly symmetric, highly branched hydrocarbon, 2,2,3,3-tetramethylbutane. If one postulates C–H bond insertion, there are no β hydrogens to transfer, so these pathways are closed to this particular species and C–C insertions appear to dominate. There are two different C–C bonds in this compound. Insertion into the terminal C–C bonds leads to reactions 37 and 40. Reaction 37 results from insertion into the C–C bond, followed by elimination of the methyl radical and concluded by a β-hydride shift to form the hydroxy–iron–olefin ion. This can transfer another hydrogen to the metal, creating the π-allyl ligand. This species can then eliminate water, creating the product in reaction 40. Products from reactions 38 and 39 result from insertion into the central C–C bond. The hydroxy–iron–isobutene complex is formed by elimination of *tert*-butyl radical and a β-hydride transfer. The Fe^+–isobutene ion is formed by two successive β-hydride transfers and elimination of water and an isobutene ligand.

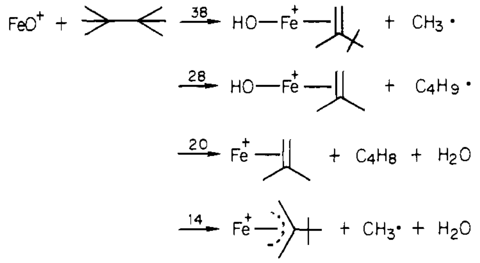

(37)
(38)
(39)
(40)

Conclusions

In general from the reactions observed, it appears that FeO^+ is more reactive toward alkanes than Fe^+ which is due mainly to the greater reaction exothermicity involved in H_2O loss. The majority of the products observed may be explained by initial C–H insertion and loss of H_2O to produce an activated Fe^+–olefin complex which subsequently decomposes. An alternative mechanism involving C–C insertion, however, cannot be ruled out and is in fact supported by observation of radical-loss products. These radical-loss products dominate for systems in which C–H insertion pathways are inhibited by the absence of β hydrogens. These species consist of stable hydroxyalkene ions which can rearrange to the aquo–π-allyl form under collisional activation.

Acknowledgment is made to the Division of Chemical Sciences in the Office of Basic Energy Sciences in the United States Department of Energy (Contract DE-AC02-80ER10689) for supporting this research and the National Science Foundation (CHE-8002685) for providing funds for the purchase of the FTMS. We also gratefully thank Marc Wise, Chemistry Department, Purdue University, for construction of the 5.2-cm cubic trapping cell.

Registry No. FeO^+, 12434-84-3; CH_4, 74-82-8; C_2H_6, 74-84-0; C_3H_8, 74-98-6; C_4H_{10}, 106-97-8; pentane, 109-66-0; hexane, 110-54-3; cyclopropane, 75-19-4; cyclobutane, 287-23-0; cyclopentane, 287-92-3; cyclohexane, 110-82-7; methylcyclohexane, 108-87-2; 2-methylpropane, 75-28-5; 2-methylbutane, 78-78-4; 2,2-dimethylpropane, 463-82-1; 2,3-dimethylbutane, 79-29-8; 2,2-dimethylbutane, 75-83-2; 2,2,3,3-tetramethylbutane, 594-82-1.

The Ionic Hydrogen Bond and Ion Solvation. 1. $NH^+\cdots O$, $NH^+\cdots N$, and $OH^+\cdots O$ Bonds. Correlations with Proton Affinity. Deviations due to Structural Effects

Michael Meot-Ner (Mautner)

Contribution from the Chemical Kinetics Division, Center for Chemical Physics, National Bureau of Standards, Washington, D.C. 20234. *Received May 10, 1982*

Abstract: In dimers $BH^+\cdots A$, a linear correlation is found between the bond dissociation energy ΔH°_D and the difference ΔPA between the proton affinities of the proton donor B and the proton acceptor A. The correlation applies for 48 $-NH^+\cdots O-$ dimers including a series with varying A and constant B, i.e., hydrates of ammonium and pyridium ions ($-NH^+\cdots OH_2$); a series with varying B and constant A, i.e., complexes $CH_3NH_3^+\cdots O-$; and other dimers with ΔPA values varying from 9 to 70 kcal mol and bond energies from 27 to 12 kcal mol^{-1}. The correlation ΔH°_D (kcal mol^{-1}) = $\Delta H^\circ_D(0) - b\Delta PA$ for $-NH^+\cdots O-$ bonds yields the parameters $\Delta H^\circ_D(0)$ = 30.0 kcal mol^{-1} and b = 0.26. Analogous linear correlations are observed for $-NH^+-\cdots N-$ bonds in a set of 8 ammonium ion dimers, and for $-OH^+\cdots O-$ bonds in a set of 21 oxonium ion hydrates, with parameters $\Delta H^\circ_D(0)$ = 23.2, b = 0.23 and ΔH°_D = 30.4, b = 0.30, respectively. Analogous linear correlations apply also for $-NH^+\cdots S-$ and $-SH^+\cdots O-$ bonds. The correlations are in accord with trends predicted by ab initio calculations of Desmeules and Allen.[1] The correlations are reliable predictors of $BH^+\cdots A$ energies within experimental error limits. Deviations from the correlations help to identify special structural effects. Such effects include multiple hydrogen bonding, intramolecular hydrogen bonding, resonance, and steric crowding.

Introduction

The thermochemistry of numerous hydrogen-bonded dimer ion $BH^+\cdot A$ has been investigated by Kebarle and other workers.[2] Bond dissociation energies (ΔH°_D) and entropies (ΔS°_D) were obtained from the temperature dependence of the equilibrium constants of clustering reactions:

$$BH^+ + A \rightleftarrows BH^+\cdot A$$

The dissociation energies range from 8 to over 30 kcal mol^{-1}. The

---

(1) Desmeules, P. J.; Allen, L. C. *J. Chem. Phys.* **1980**, *72*, 4731.
(2) Kebarle, P. *Annu. Rev. Phys. Chem.* **1977**, *28*, 445.